

Physically-Based Model of Photographic Effects for Night and Day Scenes

Roman Ďurikovič *,
Konstantin Kolchin

Computer Graphics Laboratory, Software Department, The University of Aizu,
Ikki-machi, Aizuwakamatsu-shi, Fukushima, 965 8580 Japan.

voice: [+81](242)37-2641; fax: [+81](242)37-2706

e-mail: roman,kvkol@u-aizu.ac.jp

Abstract

The light scattering within the camera system, and film emulsion and diffraction on stops and filters creates the effects of bloom and corona with radial streaks of light around high intensity objects. In the proposed digital filters, we take into account known physical effects in simulation of camera bloom and corona for realistic image synthesis. Our method is applied to the image with correctly calculated luminance values, so we reproduce the photo camera glare in a physically correct manner.

1 Introduction

The limited range of CRTs prevents the display of luminaires at their actual luminance values. Taking into account the refraction, diffraction and specular distributions will create the blooming and coronas around the luminaires. The movie production often uses the special lenses to create effects around lights or explosions. First models used in digital image synthesis to add glare effects were proposed by Nakamae *et al.* [5] and improved by Rokita [6]. They have used the Eqs. 1,2 from next section as kernels in convolution image filtering. Vos [8] defined a point spread function that describes the redistribution of point source energy

onto the visual field of a human eye. The physical mechanisms and physiological causes of glare in human vision were studied by Spencer [4]. The above works focus mostly on human perception and do not account for visual masking effects of glare. Physical properties on camera image formation system was studied in astronomy for film calibration purposes. The first definition of analytical kernel and the effect of camera bloom on emulsion grain was investigated by astronomers [7].

Our approach has been to model the physical effects caused by the camera optical system and the film emulsion for computer animation purposes. We will derive the digital filters for bloom and corona camera effects using the known physical equations. Our focus is in digital simulation of optical filter or single camera stop effects for artists, architects and urban designers used to emphasize the light scenes of the virtual buildings. Since our rendered images consist of physically correct scalar luminance values we can reproduce the correct camera effects.

2 Camera physical effects

Let us consider a simplified optical formation system consisting of optical filter, lens and projection plane positioned along the z coordinate axis while projection plane is coincident with xy plane as shown in Fig. 1. Among the rays reaching the surface of the diaphragm only the rays passing through a diaphragm arrive at its focal plane or film plate.

*On leave from Department of Computer Graphics and Image Processing, Faculty of Mathematics, Physics and Computer Science, Comenius University, Bratislava, Slovakia

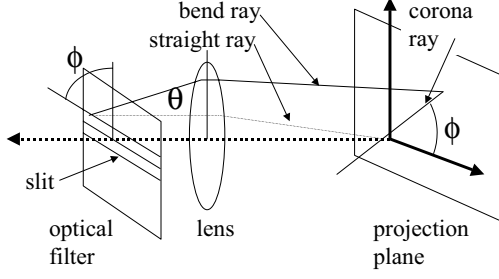


Figure 1: Camera image formation system.

2.1 Diffraction due to single diaphragm

All parallel beams passing through the lens are focused on a single point of the plane placed at the focal distance from the lens. A single small hole also called diaphragm placed before the lens creates the diffraction pattern at the projection plane which is the same pattern regardless of the location of the hole. If the diameter of hole is e , then it can be replaced by a slit with width e .

If rays with wavelength λ pass through the slit with width e , they deviate from the direct path about an angle θ . The intensity, I_s , in the diffraction pattern depends on angle θ as follows [2]:

$$I_s(\theta) = I_0 \frac{\sin^2 \alpha}{\alpha^2}, \quad (1)$$

where I_0 is the light intensity for $\theta = 0$, and

$$\alpha = \pi \frac{e}{\lambda} \sin \theta.$$

Note that the above equation describes the fact that the smaller is the slit width, the larger will be the diffraction pattern. The same is true for a hole.

2.2 Multiple holes of the same size

For many small holes distributed randomly, the diffraction pattern on the focal plane will be given by superposition of diffraction patterns coming from all particular holes. The problem of N regularly distributed holes with radius e and spacing d can be again replaced by a set of N parallel slits with width e and slit spacing d . The intensity, I_m , in the diffraction pattern given by multiple slits depends on deviation angle θ as follows:

$$I_m(\theta) = I_0 f \frac{\sin^2(e\alpha)}{(e\alpha)^2}, \quad (2)$$

where I_0 is the light intensity for $\theta = 0$, and

$$f = \frac{\sin^2(Nd\alpha)}{\sin^2(d\alpha)} \quad (3)$$

$$\alpha = \frac{\pi}{\lambda} \sin \theta. \quad (4)$$

Note, that if the slit spacing is irregular and the number of slits is big, then $f \approx N$, and the diffraction pattern is given by

$$I_m(\theta) = NI_s(\theta).$$

Therefore, the N holes of the same size and shape, will produce the diffraction pattern of a single hole amplified N times.

2.3 Diffraction on a slit network

The slit networks produce the corona diffraction pattern. Generally, the slit forming even sided polygon gives the star diffraction pattern with the same number of rays, unlike the slit forming odd sided polygon network which gives the star pattern with double number of rays as sides of polygon. Many camera filters available on the market produce corona patterns having the convergent rays with that same length. An example of a photo shot with rectangular slit network is shown in Figure 2 top.

2.4 Diffraction on camera stop

Camera stop is a hole with polygonal shape controlling the amount of light coming to the surface of the film. It is possible to produce the corona and bloom effect with a simple camera without any filter just by setting the stop and expose time. The real photograph of a scene shot during the day is shown in Figure 2 bottom. The Babinet's law claims that a hole of the same shape is always giving the same diffraction pattern. As a result we should see the same pattern for given camera settings. Number of rays in corona pattern produced by a hole obeys the similar rule as the slit network. For example, the triangular hole will always give a diffraction pattern the star with six rays, a square hole will give the star with four rays, ... [3]. The stop on camera objective used to shoot the photo had seven sided diaphragm, which explains why

we see 14 rays in corona. Investigating the Fig. 2 bottom further one can see that the rays have the random length and are divergent.



Figure 2: Real photographs: left) shot with a filter having the triangular grid of scratches rightm) shot with an objective having the 7 sided stop.

2.5 Camera Bloom

This effect is attributed to the scattering of light in the optical system where the scatter contributions from lens and small particles within the film emulsion occur in roughly equal portions. Multiple scattering within the emulsion will occur from grain to grain until it is absorbed or leaves the emulsion. Figure 3 illustrates the situation when scattered light inside the camera is added to the light coming from object B . As result, the object B is blurred and its contrast decreases.

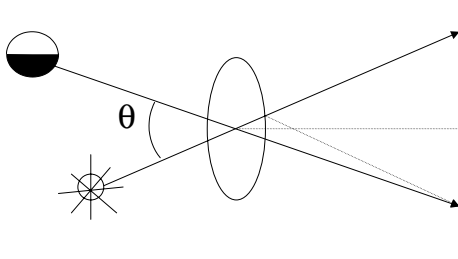


Figure 3: Camera bloom that results in reduction in contrast from scattered light.

3 Model of camera bloom and corona

This section will derive the equations that can be used to generate the digital image filters for bloom and corona camera effects. Derived filters based on known physical equations have parameters with intuitive physical meaning and can create wide range of camera effects.

Vos [8] defined a density function on the visual field that describes how a unit volume point source is “spread” onto other points of the visual field. The density function, $P(\theta)$, defined on the hemisphere of directions entering the camera is called the *point spread function* (PSF) and has the following form

$$P(\theta) = a\delta(\theta) + \frac{k}{f(\theta)},$$

where $\delta(\theta)$ is a delta function representing an ideal PSF with all energy in one point, a is the fraction of light that is not scattered, θ is the angle from the gaze direction, k is a constant between 3 and 50, and $f(\theta)$ is function of θ^n with $n \in (1.5, 3)$. Any PSF P is nonnegative and must satisfy the normalization condition on the hemisphere of directions entering the camera, where ϕ is the angle around the gaze direction and θ is the angle from the gaze direction measured in radians. Thus the function P conserves the energy in other words the energy is redistributed but not emitted or absorbed:

$$\int_0^{2\pi} \int_0^{\frac{\pi}{2}} P(\theta) \sin \theta d\theta d\phi = 1.$$

3.1 Alternative PSF definition

PSF is a nonnegative function defined in polar coordinates

$$P(r, \phi) = (1 - \varepsilon)\delta(r) + \varepsilon f(r, \phi), \quad (5)$$

satisfying the normalization condition of unique volume integral in polar coordinates:

$$\int_0^{2\pi} \int_0^\infty P(r, \phi) r dr d\phi = 1.$$

In above equations $\delta(r)$ is a delta function, r is a distance from the center of PSF located at the

gaze direction, ϕ is the angle around the gaze direction in radians, ε defines a fraction of light that is spread to neighboring points of camera visual field, $f(r, \phi)$ is a function that determines the camera effect namely bloom or corona.

3.2 Adding the Bloom

It is now desirable to find a simple general analytical formula which quantitatively represents the observed bloom spread profile. Such a function $f(r, \phi) \equiv f_b(r, \phi)$ in PSF definition, Eq. 5, is

$$f_b(r, \phi) = \frac{\varepsilon}{(1 + (r/R)^2)^\beta}, \quad (6)$$

where parameter $R \approx 30 - 120\mu m$ controls the filter width, and $\beta \approx 3 - 5$ is a constant. After substitution of Eq. 6 in to the PSF definition, Eq. 5 we derive the extension of Moffat kernel [7] which is obtained for $\varepsilon = 1$ by enhancing the energy for nearly orthogonal incident rays. For $\varepsilon = 0$ all light energy is concentrated in one single point and there is no bloom effect.

3.3 Adding the Corona

The corona effect that can simulate the randomness in the length, width and intensity fade out of corona rays is proposed to be $f(r, \phi) \equiv f_c(r, \phi)$ in Eq. 5 as follows:

$$f_c(r, \phi) = Cl(r) \cos\left(\frac{k\phi}{2}\right)^{n(r)}, \quad (7)$$

where C is a normalization constant, k is the number of rays in visible corona. The fadeout effect of rays and their length in corona is suggested to be

$$l(r) = e^{-\sigma r/l},$$

where the mean ray length l is defined by the user and σ controls the intensity fadeout along the ray. To simulate more realistic effects namely random length of rays in corona, l can be considered as a statistical variable with a given mean and deviation. In our implementations the deviation is 25% of the mean, which produce the reasonable camera spot effects.

Let w be a ray width and s be a parameter defining the convergence and divergence angle of corona

rays. Function $n(r)$ that determines whether the corona ray width converges or diverges is proposed as follows

$$n(r) = -\frac{1}{\ln(\cos \omega)},$$

where

$$\omega = \left(\frac{r}{w}\right)^{s-1}.$$

The width of rays is constant for $s = 0$, alternatively it will converge and diverge for $s < 0$ and $s > 0$, respectively. Thin and long rays can be used to simulate the corona effects of optical filters while the long and divergent rays are good for simulation of corona effects produce by the camera stop.

3.4 Implementation

The above PSFs are applied as a postprocessing to the image $I(x, y)$ of luminance distributions in cd/m^2 . The Cartesian coordinates (x, y) are the discrete image coordinates i.e. pixels. The modified luminance intensities $I'(x, y)$ of the image are then calculated by the standard discrete convolution method

$$I'(x, y) = \sum_{x_0, y_0} I(x_0, y_0) * K(x - x_0, y - y_0),$$

where $K(x, y)$ is the filter kernel derived from PDF by transforming it from polar coordinates to the Cartesian coordinate system:

$$K(x, y) = P(\sqrt{x^2 + y^2}, \tan^{-1}(\frac{y}{x})).$$

The normalization coefficient in the above PDFs can be calculated analytically or if it is not possible they can be approximated in discrete Cartesian space by using the normalization condition

$$\sum_{x, y} K(x, y) = 1.$$

The filters are independent of a particular image and their size is determined relative to the image width and height. Note that the filter is applied at each of bright points whose luminance is greater than the threshold value.



Figure 4: Camera bloom: left) the filter profile center) the scene without any effects right) the scene luminaries enhanced by a bloom effect.

4 Results and Discussion

Since, it is possible to control the spreading fraction of energy independently from decay rate in Eq. 6, the PSF can have a uniform delta peak in the center with energy at large distance from center. The filter shape with parameters $\varepsilon = 0.005$, $\beta = 2$ and $R = 10.4$ pixels is demonstrated in the left of Figure 4. The bloom effect using the same parameters is shown in right of Figure 4. Central image in Figure 4 shows the scene with original luminaries.

Figure 5 shows the simulation of camera effect on the stop with 7 sides resulting in 14 rays. On the left image of Figure 5 we show the corona filter profile using the parameter $\varepsilon = 0.005$, the ray length is set to $l = 15.6$, the number of rays is $k = 14$, and the divergence parameter is $s = 1$. Central figure shows the scene that was post-processed by the PSF using the same parameter set, the right figure shows the composition of both the corona and bloom effects.

Different camera coronas can be produced by width and divergence parameters. On Figure 6 from left first image uses convergent rays with parameters $s = -1$, $w = 10$; next image simulates the effects produced by an optical filter using the constant width rays $s = 0$, $w = 3$; the third image uses $s = 0.5$ $w = 3$ and divergent rays are shown on the last image for $s = 1$, $w = 3$. The length of ray used was approximately $l = 80$ pixels and the random factor was omitted in this figure.

5 Conclusion

We have presented the mechanisms generally accepted by the film and camera community that are responsible for a corona and bloom effects in the camera image formation system. We have focused namely on scattering in the optical filter, lens, stop and film emulsion.

We have proposed the point spread function that can be converted into the digital filter to add the bloom effect to the image simulating the scattering within the film emulsion. Similarly the PSF simulating the both the divergent and convergent effects of corona was proposed. The performed experiments indicates that the camera effects improve the image perception and can be calculated in a reasonable time of up to 1 minute. The scalar luminance images were used in our examples.

Acknowledgments

The authors thank Silvester Czanner and Edward Kopylov for their real photos with corona effects, Carl Vilbrandt for modeling the Sazaedo building. The images were rendered by the Inspirer ray tracing program developed by Integra, Inc. The author also thank Sergey Ershov for coding this method. This research was sponsored by grants from the Fukushima Prefectural Foundation in Japan for the Advancement of Science and Education.

References



Figure 5: Camera corona: left) the filter profile center) the scene with only corona effect applied on luminaries right) the scene luminaries are enhanced by both corona and bloom effects.



Figure 6: Camera corona parameters.

- [1] G. Simpson. "Ocular halos and coronas." *British Journal of Ophthalmology*, vol. 37, pp. 450-486, 1953.
- [2] M. Born E. Wolf. "Principles of optics." *Pergamon Press*, New York, 1953.
- [3] G.B. Parrent B.J. Thompson. "Physical optics notebook." *Society of Photo-optical Instrumentation Engineers*, Billingham, MA, 1969.
- [4] G. Spencer, P. Shirley, K. Zimmerman, D.P. Greenberg. "Physically-based glare effects for digital images." *In Computer Graphics Proceedings, Annual Conference Series*, pp. 325-334, ACM Siggraph, 1995.
- [5] E. Nakamae, K. Kaneda, T. Okamoto, T. Nishita. "A lighting model aiming at the drive simulators." *Computer Graphics*, vol. 24, no. 3, pp. 395-404, Siggraph'90, 1990.
- [6] P. Rokita. "A model for rendering high intensity lights." *Computer and Graphics*, vol. 17, no. 4, pp. 431-437, 1993.
- [7] A.F.J. Moffat. "A theoretical investigation of focal stellar images in the photographic emulsion and applicaiton to photographic photometry." *Astronomy and Astrophysics*, vol. 3, pp. 455, 1967.
- [8] J. Vos. "Disability glare- a state of the art report." *C.I.E. Journal*, vol. 3, no. 2, pp. 39-53, 1984.